

Topological Dirac surface states in ternary compounds $GeBi_2Te_4$, $SnBi_2Te_4$ and $Sn_{0.571}Bi_{2.286}Se_4$

Yunlong Li(李云龙), Chaozhi Huang(黄超之), Guohua Wang(王国华), Jiayuan Hu(胡佳元), Shaofeng Duan(段绍峰), Chenhang Xu(徐晨航), Qi Lu(卢琦), Qiang Jing(景强), Wentao Zhang(张文涛), and Dong Qian(钱冬)

Citation: Chin. Phys. B, 2021, 30 (**12**): 127901. DOI: 10.1088/1674-1056/ac2b92
Journal homepage: http://cpb.iphy.ac.cn; http://iopscience.iop.org/cpb

What follows is a list of articles you may be interested in

High-resolution angle-resolved photoemission study of oxygen adsorbed Fe/MgO(001)

Mingtian Zheng, Eike F. Schwier, Hideaki Iwasawa, Kenya Shimada
Chin. Phys. B, 2020, 29 (**6**): 067901. DOI: 10.1088/1674-1056/ab9196

Transport properties of doped Bi_2Se_3 and Bi_2Te_3 topological insulators and heterostructures

Zhen-Hua Wang(王振华), Xuan P A Gao(高翾), Zhi-Dong Zhang(张志东)
Chin. Phys. B, 2018, 27 (**10**): 107901. DOI: 10.1088/1674-1056/27/10/107901

In-situ spectroscopic studies and interfacial engineering on FeSe/oxide heterostructures: Insights on the interfacial superconductivity

Peng Rui, Xu Hai-Chao, Feng Dong-Lai
Chin. Phys. B, 2015, 24 (**11**): 117902. DOI: 10.1088/1674-1056/24/11/117902

Temperature effect on the electronic structure of Nb:$SrTiO_3$ (100) surface

Zhang Shuang-Hong, Wang Jia-Ou, Qian Hai-Jie, Wu Rui, Zhang Nian, Lei Tao, Liu Chen, Kurash Ibrahim
Chin. Phys. B, 2015, 24 (**2**): 027901. DOI: 10.1088/1674-1056/24/2/027901

Mn overlayers on PbTe (111): Substitutional adsorption and interface formation

Wu Hai-Fei, Zhang Han-Jie, Lu Yun-Hao, Yan Yong-Hong, Li Hai-Yang, Bao Shi-Ning, He Pi-Mo
Chin. Phys. B, 2014, 23 (**12**): 127901. DOI: 10.1088/1674-1056/23/12/127901

RAPID COMMUNICATION

Topological Dirac surface states in ternary compounds $GeBi_2Te_4$, $SnBi_2Te_4$ and $Sn_{0.571}Bi_{2.286}Se_4$*

Yunlong Li(李云龙)[1], Chaozhi Huang(黄超之)[1], Guohua Wang(王国华)[1], Jiayuan Hu(胡佳元)[1], Shaofeng Duan(段绍峰)[1], Chenhang Xu(徐晨航)[1], Qi Lu(卢琦)[1], Qiang Jing(景强)[1], Wentao Zhang(张文涛)[1,†], and Dong Qian(钱冬)[1,2,‡]

[1] *Key Laboratory of Artificial Structures and Quantum Control (Ministry of Education), Shenyang National Laboratory for Materials Science, School of Physics and Astronomy, Shanghai Jiao Tong University, Shanghai* 200240, *China*

[2] *Tsung-Dao Lee Institute, Shanghai Jiao Tong University, Shanghai* 200240, *China*

(Received 4 July 2021; revised manuscript received 4 September 2021; accepted manuscript online 30 September 2021)

Using high-resolution angle-resolved and time-resolved photoemission spectroscopy, we have studied the low-energy band structures in occupied and unoccupied states of three ternary compounds $GeBi_2Te_4$, $SnBi_2Te_4$ and $Sn_{0.571}Bi_{2.286}Se_4$ near the Fermi level. In previously confirmed topological insulator $GeBi_2Te_4$ compounds, we confirmed the existence of the Dirac surface state and found that the bulk energy gap is much larger than that in the first-principles calculations. In $SnBi_2Te_4$ compounds, the Dirac surface state was observed, consistent with the first-principles calculations, indicating that it is a topological insulator. The experimental detected bulk gap is a little bit larger than that in calculations. In $Sn_{0.571}Bi_{2.286}Se_4$ compounds, our measurements suggest that this nonstoichiometric compound is a topological insulator although the stoichiometric $SnBi_2Se_4$ compound was proposed to be topological trivial.

Keywords: angle-resolved photoemission spectroscopy, band structure, topological insulator, ternary compounds

PACS: 79.60.−i, 71.20.−b, 73.20.At, 74.70.Dd **DOI:** 10.1088/1674-1056/ac2b92

1. Introduction

Topological insulators have inspired enormous interests in the last decade.[1–12] The novel electronic state of TIs with strong spin–orbit coupling is characterized by the bulk band gap and spin-split helical Dirac surface state that is protected from backscattering on defects by the time reversal symmetry. Topological insulator was first realized in the $Bi_{1-x}Sb_x$ alloy with the very complicated topological surface state observed by angle-resolved photoemission spectroscopy (ARPES).[13] Later on, the novel surface state with a single helical Dirac cone was observed in some layered binary compounds, such as Bi_2Te_3 and Bi_2Se_3 by ARPES,[14–16] which makes topological insulator's surface state be potentially useful in the topological quantum computation, spintronics and so on.[17–23] Searching for new topological insulators is still of interests for future applications.

Besides the binary compounds, a large homologous family of ternary compounds $A^{IV}B^{VI}$–$mA^{V}_2B^{VI}_3$ (A^{IV} = Ge, Sn, Pb; A^{V} = Bi, Sb; B^{VI} = Te, Se) have been theoretically studied by the first-principles calculations based on the density functional theory (DFT) on their topological properties. Most of them were predicted to be topological insulators.[24,25] It is well-known that standard DFT calculations underestimate the band gap for fundamental reasons.[26] Sometimes this deficiency of DFT causes incorrect predictions of the topological phase and additional perturbation theory needs to be applied.[27] Therefore, the direct measurement of the band structure by ARPES is also crucial to determine the topological phase as well as the bulk energy gap in the ternary compounds. Recently, some of those ternary compounds have been studied by ARPES, such as $PbBi_4Te_7$,[24] $GeBi_2Te_4$[28,29] and Bi_2Te_2Se.[28] With the observation of the Dirac surface state, they were verified to be topological insulators.

In this work, we studied the low-energy electronic structure both in occupied and unoccupied states near Fermi level of three ternary compounds $GeBi_2Te_4$,[30] $SnBi_2Te_4$[30] and $Sn_{0.571}Bi_{2.286}Se_4$[31,32] single crystals by ARPES and time-resolved (pump–probe) ARPES (tr-ARPES). $GeBi_2Te_4$ has already confirmed to be a topological insulator.[28] Its bulk energy gap was accessed by surface alkali deposition (surface electron doping). However, sometimes the surface alkali deposition could change the band structure due to the electric field effect,[33] we carried out tr-ARPES to directly probe the unoccupied state in $GeBi_2Te_4$ without any surface doping. Our experiments find that its bulk energy gap is much larger than that in calculations. So far, $SnBi_2Te_4$ and $Sn_{0.571}Bi_{2.286}Se_4$ compounds have not been studied. In our experiments, surface Dirac cone is observed both in $SnBi_2Te_4$

*Project supported by the National Natural Science Foundation of China (Grant Nos. 11521404, 12074248, 11974243, and 11804194). D. Q. and W. T. Z. acknowledge additional support from a Shanghai talent program.

†Corresponding author. E-mail: wentaozhang@sjtu.edu.cn

‡Corresponding author. E-mail: dqian@sjtu.edu.cn

© 2021 Chinese Physical Society and IOP Publishing Ltd

and $Sn_{0.571}Bi_{2.286}Se_4$, suggesting that they are both topological insulators.

2. Methods

Single crystals of $SnBi_2Te_4$ compound were grown by self-flux method with stoichiometric mixtures of high-purity (99.99%) elements Sn, Bi, and Te. Mixtures sealed in a quartz tube were heated to 600 °C and then cooled to room temperature at a rate of ∼ 10 °C/h after two days. Single crystals of $GeBi_2Te_4$ and $Sn_{0.571}Bi_{2.286}Se_4$ compounds were synthesized by chemical vapor transport method with transport agent I_2. High-purity (99.99%) powders of pure elements (Ge:Bi:Te = 1:2:4 and Sn:Bi:Se = 1:4:7) and a spot of iodine were mixed and sealed into a quartz tube. Temperature gradient was set from 900 °C to 800 °C and 550 °C to 450 °C in a two-zone furnace for $GeBi_2Te_4$ and $Sn_{0.571}Bi_{2.286}Se_4$, respectively.

Synchrotron-ARPES measurements were performed at the ARPES beamline in National Synchrotron Radiation Laboratory (Hefei) and the Dreamline in Shanghai Synchrotron Radiation Facility. The tr-ARPES measurements were carried out using a 6.05 eV probe laser and an infrared 1.77 eV pump laser (30 fs and 500 kHz).[34,35] Energy resolution is better than 10 meV for normal ARPES and 20 meV for tr-ARPES. Angular resolution is better than 2% of the Brillouin zone. Time resolution of tr-ARPES is about 130 fs. All samples were cleaved *in situ*. Spectra were collected at 20 K for normal ARPES and 4 K for tr-ARPES with chamber pressure better than 1×10^{-10} Torr.

3. Results and discussion

3.1. $GeBi_2Te_4$

Figure 1(a) presents the crystal structures of Bi_2Te_3 and $GeBi_2Te_4$. In Bi_2Te_3, the unit cell is composed of three quintuple layers. Similar to Bi_2Te_3, the unit cell of $GeBi_2Te_4$ can be represented by the stacking of three septuple layers along *c*-axis.[28] The difference between $GeBi_2Te_4$ and Bi_2Te_3 is that the middle Te-layer in the Bi_2Te_3's quintuple layer is replaced by a Te–Ge–Te sandwich. Single crystal x-ray diffraction (XRD) spectra of $GeBi_2Te_4$ shows sharp $(00l)$ peaks in Fig. 1(b), indicating good crystallinity.

Figure 1(c) shows the calculated band structures of $GeBi_2Te_4$ in previous work.[24] According to calculations, $GeBi_2Te_4$ is topologically nontrivial. Shaded area and red curves in Fig. 1(c) are the bulk band projections and the surface states, respectively. Above the Fermi level, the bulk conduction band projection divides into two branches that are separated in momentum. At $\bar{\Gamma}$ point, the energy gap between two branches is about 0.05 eV. The surface Dirac cone is within

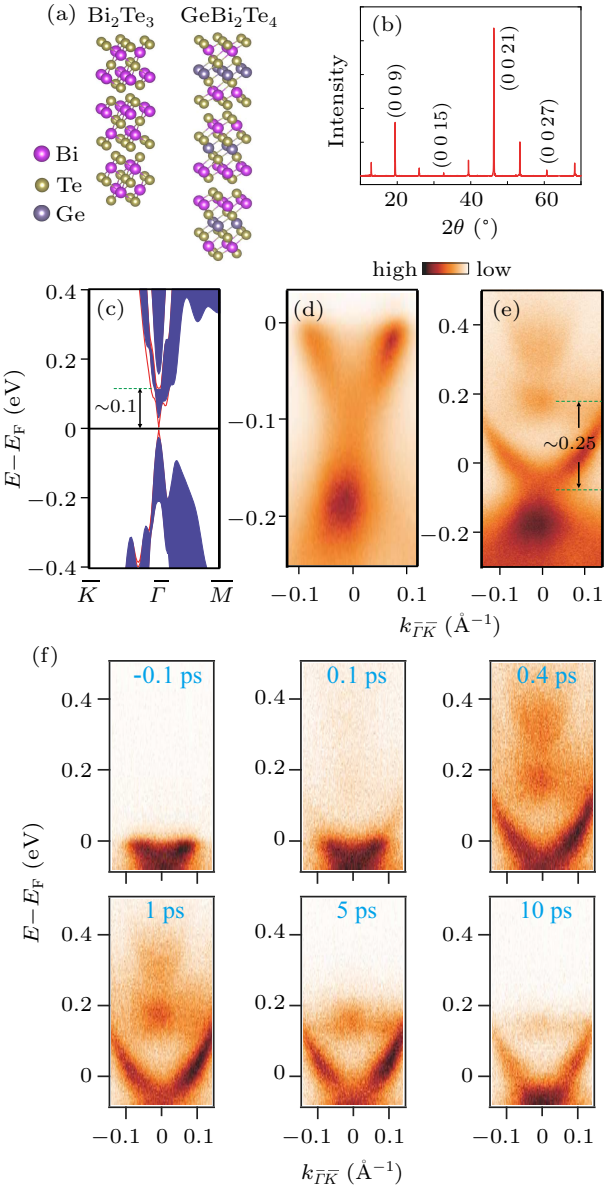


Fig. 1. (a) Crystal structure of Bi_2Te_3 and $GeBi_2Te_4$. (b) Single crystal XRD of $GeBi_2Te_4$ compound. Sharp $(00l)$ diffraction peaks were detected. (c) Calculated band structure of $GeBi_2Te_4$ from Ref. [24]. $\Delta k_{\bar{\Gamma}-\bar{K}} = 1.03$ Å^{-1}. Shaded area is the bulk band projection. Red curves are the surface states. Dirac point well separates from the bulk band projection. (d) ARPES spectra along $\bar{K}-\bar{\Gamma}-\bar{K}$ direction. Incident photon energy is 6.05 eV. (e) Tr-ARPES spectra at a delay time of ∼ 0.4 ps. Conduction band above the Fermi level is observed. (f) Tr-ARPES spectra for $GeBi_2Te_4$ at different delay times. The decay of the bottom part of the conduction bands and the surface band is very slow.

the bulk band gap and the Dirac point separates from the bulk band projection. The calculated bulk gap is ∼ 0.06 eV. Figure 1(d) presents ARPES spectra along $\bar{K}$–$\bar{\Gamma}$–$\bar{K}$ direction using incident photons of 6.05 eV. Topological surface state with linear band dispersion is observed, consistent with the previous results[28,29] except that the Dirac point in our sample is much closer to the Fermi level. The tr-ARPES measurements can be used to probe the unoccupied states to check the bulk band gap.[36–38] The tr-ARPES spectra at the delay time 0.4 ps is presented in Fig. 1(e). Spectra weight above the Fermi level is observed. There are two branches of spectral

weight. The lower branch locates roughly between ∼ 0.15 eV and ∼ 0.25 eV, and the upper branch locates above ∼ 0.25 eV. The energy separation between the two branches at $\bar{\Gamma}$ point is close to 0.05 eV. Qualitatively, the observed spectral weight above the Fermi level in Fig. 1(e) is consistent with the bulk conduction band.

Furthermore, in Fig. 1(f), we present six tr-ARPES spectra with various pump-probe delays. At the negative delay time (before pumping), there is no spectral weight above the Fermi level. At a delay time of 0.1 ps, there appears spectral weight above the Fermi level. At a delay time of 0.4 ps, the V-shaped surface band as well as two branches of spectral weight becomes clearly visible. At a delay time of 5 ps, the intensity of the higher branch significantly decays. The decay of the lower branch and the surface state populations is much slower, persisting for more than 10 ps. Similar dynamics was observed in the tr-ARPES study on Bi_2Se_3 and was comprehensively discussed considering the spectral weight besides the surface band is the bulk conduction band.[36] In our sample, the electrons in the upper branch can energetically relax towards the lower branch, but the electrons in the lower branch cannot rapidly relax to low energy bulk conduction state because it is already at the bottom of the conduction band. The very long persisting time of the lower branch and the surface state population follows the same mechanism in Bi_2Se_3.[36] The slow recombination of the lower branch (bulk conduction state) population is due to the existence of the bulk band gap, which is much larger than the phonon energy. The long-lived population of the surface state is attributed to the continuous electron filling to the surface state from the bulk conduction band population. The similarity between $GeBi_2Te_4$ and Bi_2Se_3 in electron dynamics in tr-ARPES supports that our observed spectra weight above the Fermi level comes from the bulk conduction band.

In Fig. 1(e), it is ∼ 0.25 eV between the detected conduction band bottom and the Dirac point. It is worth noting that the observed conduction band bottom is not necessarily the exact conduction band minimum because the corresponding k_z in our tr-ARPES measurement may not reach the right momentum position where the conduction band minimum locates. So the experimental observed energy gap could be larger than the real bulk energy gap. Therefore, to compare with calculations, we only consider the extreme condition. We call the lower branch of the bulk conduction band projection in Fig. 1(c) the first bulk conduction projection. Marked in Fig. 1(c), the largest energy difference between the Dirac point and the first bulk conduction band projection at $\bar{\Gamma}$ point is about 0.1 eV. Even in this condition, the experimental energy gap is still about three times of the calculated value. Although the size of bulk gap is not directly related to the topological property of a material, information of the bulk gap size is useful because a small bulk band gap will bring undesired thermal excited bulk carrier that will hinder the novel property of the surface state.

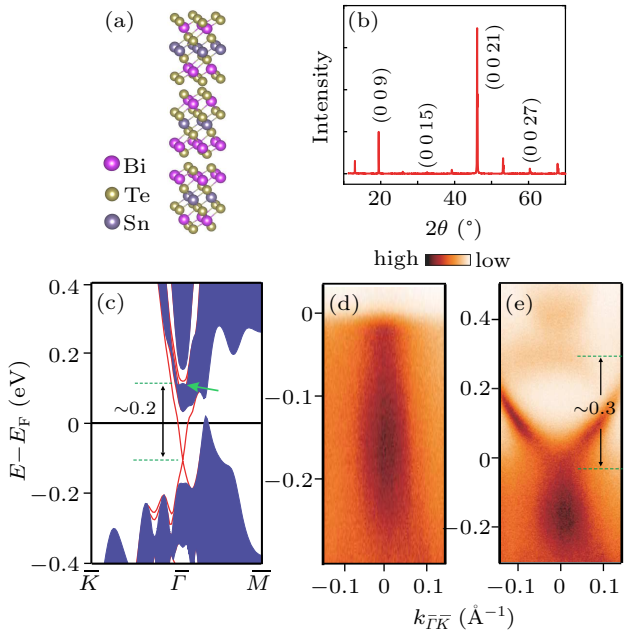


Fig. 2. (a) Crystal structure of $SnBi_2Te_4$. (b) Single crystal XRD of $SnBi_2Te_4$ compound. Sharp $(00l)$ diffraction peaks are detected. (c) Calculated band structures of $SnBi_2Te_4$ from Ref. [24]. $\Delta k_{\bar{\Gamma}-\bar{K}} = 1.01$ Å^{-1}. Dirac point overlaps with the bulk band projection in energy although they separate in momentum. Green arrow indicates the slightly downward dispersion. (d) ARPES spectra near Fermi level along $\bar{K}$–$\bar{\Gamma}$–$\bar{K}$ direction. Incident photon energy is 6.05 eV. (e) Tr-ARPES spetra at a delay time of ∼ 0.4 ps. Conduction band above the Fermi level is observed.

3.2. $SnBi_2Te_4$

Substituting Sn for Ge atoms, $SnBi_2Te_4$ is isostructural with $GeBi_2Te_4$, shown in Fig. 2(a). Figure 2(b) shows the single crystal XRD spectra with $(00l)$ diffraction peaks of single crystalline $SnBi_2Te_4$. The calculated band structure of $SnBi_2Te_4$ in previous work[24] is shown in Fig. 2(c). According to the calculations, $SnBi_2Te_4$ is topologically nontrivial. Unlike $GeBi_2Te_4$, $SnBi_2Te_4$ is an indirect band-gap semiconductor and most of its topological surface state including the Dirac point is overlapped with the bulk valance band projection in energy although they separate in momentum. The calculated bulk gap is ∼ 0.01 eV.

Band dispersion along $\bar{K}$–$\bar{\Gamma}$–$\bar{K}$ is plotted in Fig. 2(d). Experimentally, it is unclear whether there is Dirac surface state or not. To clarify, we carried out tr-ARPES to probe the unoccupied bands above the Fermi level. The tr-ARPES spectra at a delay time of 0.4 ps is shown in Fig. 2(e). Now Dirac surface state is clearly observed, consistent with the DFT calculations. The Dirac point in $SnBi_2Te_4$ is very close to the Fermi level. Therefore, our $SnBi_2Te_4$ compound is heavily p-doped. Bulk conduction band was also detected in the tr-ARPES measurements. Consistent with the calculations, two branches of spectral weight above the Fermi level were detected. In Fig. 2(e), the lower branch shows slightly downward dispersion. In calculations, in Fig. 2(c), near the $\bar{\Gamma}$ point,

the top of the first bulk conduction band projection also shows slightly downward dispersion (indicated by the green arrow). The observation of the downward dispersion clearly indicates that our experimental accessed k_z in $SnBi_2Te_4$ is not at the position where the real conduction band minimum locates. The bottom of the detected bulk conduction band is about 0.3 eV above the Dirac point, which is comparable with the direct gap at the $\bar{\Gamma}$ point in calculations. Marked in Fig. 2(c), the largest energy difference between the Dirac point and the first bulk conduction band projection at $\bar{\Gamma}$ is about 0.2 eV.

3.3. $Sn_{0.571}Bi_{2.286}Se_4$

According to the calculations, stoichiometric compound $SnBi_2Se_4$ is a trivial insulator.[24] However, experimentally, instead of the stoichiometric ratio, previous work reported that a nonstoichimetric compound $Sn_{0.571}Bi_{2.286}Se_4$ is much more stable.[31,32] Sketched in Fig. 3(a), for the nonstoichiometric compound $Sn_{0.571}Bi_{2.286}Se_4$, the middle Ge-layer of the $GeBi_2Te_4$ septuple layer is replaced by a mixed layer (0.45 Bi/0.41 Sn/0.14 vacancies).[31,32] Because of the mixed Bi/Sn/vacancies layer in $Sn_{0.571}Bi_{2.286}Se_4$, no first-principles calculation is available. Its topological property is unclear. We carried out ARPES measurements to check its topological property. Single crystal XRD spectra of single crystalline $Sn_{0.571}Bi_{2.286}Se_4$ with sharp $(00l)$ diffraction peaks is shown in Fig. 3(b), consistent with previous report.[31,32]

ARPES spectra near the Fermi level using three different photon energies (82 eV, 14 eV and 6.05 eV) are presented in Figs. 3(c), 3(e), and 3(g), respectively. Corresponding curvature plots[39] are presented in Figs. 3(d), 3(f), and 3(h) to visualize the dispersive feature more clearly. A V-shaped band pair is observed to cross the Fermi level. Although the intensity varies, the dispersion of the observed band is very similar using different photon energies, which implies that the bands come from the surface state. The characteristics of the surface band are obtained based on the ARPES spectra using the incident photon of 6.05 eV. In Fig. 3(h), we observed a band crossing point or Dirac point (zero energy gap, indicated by the white arrow) similar to that in the typical topological insulator Bi_2Se_3.[16] Near this crossing point, the band dispersion is linear-like according to the curvature image in Fig. 3(h). In addition, we also extracted the band dispersion near the crossing point using momentum distribution curves (MDCs) in Fig. 3(i). Black dots in Fig. 3(i) mark the peak positions by MDC fitting. The band crossing point locates at ~ 0.13 eV below the Fermi level.

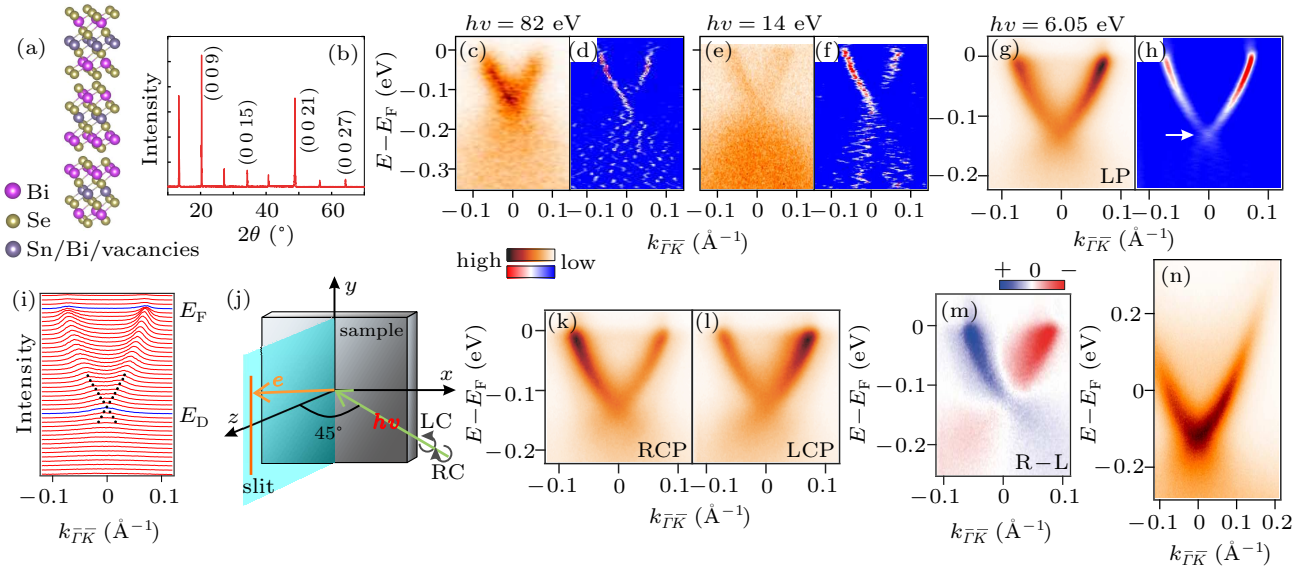


Fig. 3. (a) Crystal structure of $Sn_{0.571}Bi_{2.286}Se_4$. (b) Single crystal XRD of $Sn_{0.571}Bi_{2.286}Se_4$ compound. Sharp $(00l)$ diffraction peaks are detected. (c), (e) and (g) ARPES spectra near the Fermi level of $Sn_{0.571}Bi_{2.286}Se_4$ using incident photon energies of 82 eV, 14 eV and 6.05 eV, respectively. (d), (f) and (h) Corresponding curvature plots of (c), (e) and (g). (i) MDCs of (g). Black dots mark the peak positions from fitting. (j) Schematics of experimental geometry used for CD-ARPES measurements. The detector slit is vertical. The incident angle of the light is 45°. (k), (l) Surface Dirac band probed by right circularly polarized and left circularly polarized lights, respectively. (m) Intensity difference between ARPES spectra using right circularly polarized and left circularly polarized incident lights. Clear circular dichroism is observed. (n) Tr-ARPES spectra at a delay time of ~ 0.4 ps. No conduction band above the Fermi level is observed.

We also carried out circular dichroism (CD) experiments[40–44] on this material using the incident photon of 6.05 eV. Schematics of the experimental geometry is plotted in Fig. 3(j), which is similar to that in previous CD experiment on Bi_2Se_3.[43] The detector slit in our experiment is vertical. The incident angle of the light is about 45°. Figures 3(k) and 3(l) present ARPES spectra taken with right and left circularly polarized (RCP and LCP) lights, respectively. In Fig. 3(m), the intensity difference between ARPES spectra using RCP and LCP demonstrates the CD effect. Although the CD effect in ARPES is a complicated and developing method,[42–44] the CD effect in $Sn_{0.571}Bi_{2.286}Se_4$ could be a consequence when

this material is a topological insulator. Therefore, by combining the zero energy gap, linear-like band dispersion and CD effect, we suggest that $Sn_{0.571}Bi_{2.286}Se_4$ is a topological insulator. We also tried to detect the unoccupied bulk state above the Fermi level by the tr-ARPES experiments, shown in Fig. 3(n). Unlike $GeBi_2Te_4$ or $SnBi_2Te_4$, no bulk conduction band is observed. Maybe $Sn_{0.571}Bi_{2.286}Se_4$ has much larger bulk gap or the ARPES matrix element effect hinders the signal of the bulk conduction band. It will be studied in the future.

4. Conclusion

In summary, we carried out ARPES and tr-ARPES measurements on three ternary compounds $GeBi_2Te_4$, $SnBi_2Te_4$ and $Sn_{0.571}Bi_{2.286}Se_4$. Through the detection of Dirac-like surface state, we found that two Sn-based ternary compounds are both topological insulators besides the already known topological insulator $GeBi_2Te_4$. The unoccupied bulk conduction bands were checked directly by tr-ARPES. The observed bulk energy gap of $GeBi_2Te_4$ is much larger than the calculations, while that in $SnBi_2Te_4$ is close to the calculations. To obtain larger bulk energy gap in calculations, first-principles calculation involving GW or HSE method maybe needed. Unfortunately, we did not observed the bulk conduction band in $Sn_{0.571}Bi_{2.286}Se_4$. Our experiments enrich the topological material families and may provide more choices for future applications based on topological insulators.

References

[1] Hasan M Z and Kane C L 2010 *Rev. Mod. Phys.* **82** 3045
[2] Qi X L and Zhang S C 2011 *Rev. Mod. Phys.* **83** 1057
[3] Thouless D J, Kohmoto M, Nightingale M P and Nijs M den 1982 *Phys. Rev. Lett.* **49** 405
[4] Haldane F D M 1988 *Phys. Rev. Lett.* **61** 2015
[5] Murakami S, Nagaosa N and Zhang S C 2004 *Phys. Rev. Lett.* **93** 156804
[6] Kane C L and Mele E J 2005 *Phys. Rev. Lett.* **95** 146802
[7] König M, Wiedmann S, Brüne C, Roth A, Buhmann H, Molenkamp L W, Qi X L and Zhang S C 2007 *Science* **318** 766
[8] Qi X L and Zhang S C 2010 *Phys. Today* **63** 33
[9] Yang Z Q, Jia J F and Qian D 2016 *Chin. Phys. B* **25** 117312
[10] Liu C and Liu X R 2019 *Acta Phys. Sin.* **68** 227901 (in Chinese)
[11] Pei C, Xia Y, Wu J, Zhao Y, Gao L, Ying T, Gao B, Li N, Yang W, Zhang D, Gou H, Chen Y, Hosono H, Li G and Qi Y 2020 *Chin. Phys. Lett.* **37** 066401
[12] Zhang J, Wang D, Shi M, Zhu T, Zhang H and Wang J 2020 *Chin. Phys. Lett.* **37** 077304
[13] Hsieh D, Qian D, Wray L, Xia Y, Hor Y S, Cava R J and Hasan M Z 2008 *Nature* **452** 970
[14] Chen Y L, Analytis J G, Chu J H, Liu Z K, Mo S K, Qi X L, Zhang H J, Lu D H, Dai X, Fang Z, Zhang S C, Fisher I R, Hussain Z and Shen Z X 2009 *Science* **325** 178
[15] Hsieh D, Xia Y, Qian D, Wray L, Dil J H, Meier F, Osterwalder J, Patthey L, Checkelsky J G, Ong N P, Fedorov A V, Lin H, Bansil A, Grauer D, Hor Y S, Cava R J and Hasan M Z 2009 *Nature* **460** 1101
[16] Xia Y, Qian D, Hsieh D, Wray L, Pal A, Lin H, Bansil A, Grauer D, Hor Y S, Cava R J and Hasan M Z 2009 *Nat. Phys.* **5** 398
[17] Sato M and Ando Y 2017 *Rep. Prog. Phys.* **80** 076501
[18] Leijnse M and Flensberg K 2012 *Semicond. Sci. Technol.* **27** 124003
[19] Xu S Y, Alidoust N, Belopolski I, Richardella A, Liu C, Neupane M, Bian G, Huang S H, Sankar R, Fang C, Dellabetta B, Dai W, Li Q, Gilbert M J, Chou F, Samarth N and Hasan M Z 2014 *Nat. Phys.* **10** 943
[20] Xu J P, Wang M X, Liu Z L, Ge J F, Yang X, Liu C, Xu Z A, Guan D, Gao C L, Qian D, Liu Y, Wang Q H, Zhang F C, Xue Q K and Jia J F 2015 *Phys. Rev. Lett.* **114** 017001
[21] Sun H H, Zhang K W, Hu L H, Li C, Wang G Y, Ma H Y, Xu Z A, Gao C L, Guan D D, Li Y Y, Liu C, Qian D, Zhou Y, Fu L, Li S C, Zhang F C and Jia J F 2016 *Phys. Rev. Lett.* **116** 257003
[22] Shi H B, Yan L Q, Su Y T, Wang L, Cao X Y, Bi L Z, Meng Y, Sun Y and Zhao H W 2020 *Chin. Phys. B* **29** 117302
[23] Zhang T Y, Yan Q and Sun Q F 2021 *Chin. Phys. Lett.* **38** 077303
[24] Eremeev S V, Landolt G, Menshchikova T V, Slomski B, Koroteev Y M, Aliev Z S, Babanly M B, Henk J, Ernst A, Patthey L, Eich A, Khajetoorians A A, Hagemeister J, Pietzsch O, Wiebe J, Wiesendanger R, Echenique P M, Tsirkin S S, Amiraslanov I R, Dil J H and Chulkov E V 2012 *Nat. Commun.* **3** 635
[25] Menshchikova T V, Eremeev S V and Chulkov E V 2013 *Appl. Surf. Sci.* **267** 1
[26] Perdew J P and Levy M 1983 *Phys. Rev. Lett.* **51** 1884
[27] Autès G, Isaeva A, Moreschini L, Johannsen J C, Pisoni A, Mori R, Zhang W T, Filatova T G, Kuznetsov A N, Forró L, Van den Broek W, Kim Y, Kim K S, Lanzara A, Denlinger J D, Rotenberg E, Bostwick A, Grioni M and Yazyev O V 2016 *Nat. Mater.* **15** 154
[28] Neupane M, Xu S Y, Wray L A, Petersen A, Shankar R, Alidoust N, Liu C, Fedorov A, Ji H, Allred J M, Hor Y S, Chang T R, Jeng H T, Lin H, Bansil A, Cava R J and Hasan M Z 2012 *Phys. Rev. B* **85** 235406
[29] Sterzi A, Manzoni G, Crepaldi A, Cilento F, Zacchigna M, Leclerc M, Bugnon Ph, Magrez A, Berger H, Petaccia L and Parmigiani F 2018 *J. Electron. Spectrosc. Relat. Phenom.* **225** 23
[30] Kuznetsova L A, Kuznetsov V L and Rowe D M 2000 *J. Phys. Chem. Solids* **61** 1269
[31] Pérez Vicente C, Tirado J L, Adouby K, Jumas J C, Touré A A and Kra G 1999 *Inorg. Chem.* **38** 2131
[32] Heinke F, Urban P, Werwein A, Fraunhofer C, Rosenthal T, Schwarzmüller S, Souchay D, Fahrnbauer F, Dyadkin V, Wagner G and Oeckler O 2018 *Inorg. Chem.* **57** 4427
[33] Kim J, Baik S S, Ryu S H, Sohn Y, Park S, Park B G, Denlinger J, Yi Y, Choi H J and Kim K S 2015 *Science* **349** 723
[34] Yang Y, Tang T, Duan S, Zhou C, Hao D and Zhang W 2019 *Rev. Sci. Instrum.* **90** 063905
[35] Tang T, Wang H, Duan S, Yang Y, Huang C, Guo Y, Qian D and Zhang W 2020 *Phys. Rev. B* **101** 235148
[36] Sobota J A, Yang S, Analytis J G, Chen Y L, Fisher I R, Kirchmann P S and Shen Z X 2012 *Phys. Rev. Lett.* **108** 117403
[37] Sobota J A, Yang S L, Kemper A F, Lee J J, Schmitt F T, Li W, Moore R G, Analytis J G, Fisher I R, Kirchmann P S, Devereaux T P and Shen Z X 2013 *Phys. Rev. Lett.* **111** 136802
[38] Ito H, Otaki Y, Tomohiro Y, Ishida Y, Akiyama R, Kimura A, Shin S and Kuroda S 2020 *Phys. Rev. Res.* **2** 043120
[39] Zhang P, Richard P, Qian T, Xu Y M, Dai X and Ding H 2011 *Rev. Sci. Instrum.* **82** 043712
[40] Park S R, Han J, Kim C, Koh Y Y, Kim C, Lee H, Choi H J, Han J H, Lee K D, Hur N J, Arita M, Shimada K, Namatame H and Taniguchi M 2012 *Phys. Rev. Lett.* **108** 046805
[41] Wang Y and Gedik N 2013 *Phys. Status Solidi RRL* **7** 64
[42] Wang Y H, Hsieh D, Sie E J, Steinberg H, Gardner D R, Lee Y S, JarilloHerrero P and Gedik N 2012 *Phys. Rev. Lett.* **109** 127401
[43] Vidal F, Eddrief M, Rache Salles B, Vobornik I, Velez-Fort E, Panaccione G and Marangolo M 2013 *Phys. Rev. B* **88** 241410
[44] Kondo T, Nakashima Y, Ishida Y, Kikkawa A, Taguchi Y, Tokura Y and Shin S 2017 *Phys. Rev. B* **96** 241413